LaserSPECks: Laser SPECtroscopic Trace-Gas Sensor Networks - Sensor Integration and Applications

Stephen So, Farinaz Koushanfar, Anatoliy Kosterev, and Frank Tittel
Department of Electrical and Computer Engineering
Rice University, Houston, TX 77005
{steveso,farinaz,akoster,fkt}@rice.edu

ABSTRACT

We introduce a novel laser spectroscopic trace-gas sensor platform, LaserSPECks that integrates recently developed *miniature* quartz-enhanced photoacoustic spectroscopy (QEPAS) gas sensing technology. This *universal* platform uses infrared laser spectroscopy detect and quantify *numerous* gas species at part-per-million to part-per-billion (ppm-ppb) concentrations [2]. Traditional gas sensing devices capable of the same sensitivity and specificity are several orders of magnitude larger in size, cost, and power consumption. Thus, high resolution gas sensing technology has been difficult to integrate into small, low-power, replicated sensors suitable for wireless sensor networks (WSNs). This paper presents the principles behind laser based trace gas detection, design issues, and outlines the implementation of a miniaturized trace-gas sensor from commerical-off-the-shelf (COTS) components. We report on an early prototype as a proof-of-concept for integration into WSN applications. We also describe a number of ongoing collaborations in utilizing the platform in air pollution and carbon flux quantification, industrial plant control, explosives detection, and medical diagnosis. Furthermore, we discuss experimental performance evaluations to examine general platform requirements for these types of sensors. The results of our evaluation illustrate that our prototype improves upon previous gas sensing technology by *two orders of magnitude* in measures of power consumption, size, and cost, without sacrificing sensor performance. Our design and experiments reveal that laser-based trace-gas sensors built from COTS can be successfully implemented and integrated within WSN nodes to enable a wide range of new and important sensing applications.

Categories and Subject Descriptors

C.5.m [**Computer system implementation**]: Misc.; J.2 [**Physical sciences and engineering**]: Chemistry

IPSN'07, April 25-27, 2007, Cambridge, Massachusetts, USA.

General Terms

Performance, Design

Keywords

sensors, spectroscopy, lasers, trace gas sensing

1. INTRODUCTION

The detection and quantification of trace-gases provide a diverse set of real-world applications. In this paper, we report the first successful design and implementation of a *high-performance miniature gas sensor* integrated within the WSN methodology. The miniature gas sensor implements *quartz-enhanced photoacoustic spectroscopy* (QEPAS), a technology recently developed at Rice University [6]. The platform is *universal* since detection and quantification of any gas type is possible, as long as the laser can tune to the specific wavelengths of a particular trace-gas species. These optical techniques have extremely high specificity as compared to semiconductor/metal-oxide gas sensors (previously integrated into WSNs) which suffer from high false positive and negative rates (undesirable in security and medical applications). Thus, QEPAS sensors can be practically deployed

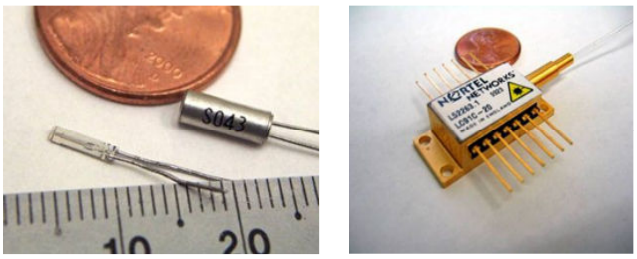

(a) (b)

Figure 1: Photograph of quartz Tuning Fork (TF) and telecom laser to indicated physical size: (a) open TF, US penny, Factory sealed tuning fork, mm scale ruler; (b) Fiber coupled telecom laser in a 14 pin butterfly DIP (dual in-line) package.

in WSNs, and will simultaneously provide sensitivity, specificity, low maintenance, no consumables, and low cost. One key enabler of QEPAS-based miniature sensors is the recent availability of compact, efficient, high optical power, mass produced near-infrared (NIR) laser sources that are based on semiconductor diode lasers and a low cost miniature sensing element depicted in Fig. 1. We present LaserSPECks,

a sensor node platform on which QEPAS electronics and a telecom diode laser are interfaced to COTS microcontroller, storage, and radio modules suitable for WSNs.

Furthermore, we describe trace-gas sensing results from an early working prototype of the LaserSPECks platform. Previously, QEPAS trace-gas sensors built from laboratory equipment have been applied to a variety of target gases, including H_2O, HCN, NH_3, CO, and CO_2. As a proof-of-concept, the prototype LaserSPECks platform successfully detects and quantifies CO_2 with comparable accuracy at low cost, handheld size, and low power. We also outline the near-term improvements that we are expecting to achieve in the next generation implementation of our sensor devices.

The availability of high resolution trace-gas sensors built from COTS will enable the macro-monitoring of gas in scales that are not currently attainable; this would in turn generate a wide variety of new high volume applications for both WSNs and trace-gas sensing. In this report, we will describe a number of applications that we are exploring in our current research initiatives, as well as potential applications that are becoming practical as cost, sensitivity, and manufacturability improve. More specifically, we describe our recent discussions with the semiconductor industry (Texas Instruments and Motorola) to implement the LaserSPECks platform for monitoring ammonia contamination in their fabrication facilities, and collaborations with the Texas Medical Center and John Hopkins School of Public Health as part of the National Science Foundation Mid-Infrared Technologies for the Health and Environment Engineering Research Center (NSF MIRTHE ERC) to utilize the platform in exhaled biomarker detection for disease diagnosis.

The remainder of the paper is organized as follows. In Section 2, we provide background about the operation of optically-based trace-gas detection. Further theory of operation for QEPAS, the main sensing technology in this work, is outlined in Section 3. Section 4 focuses on issues that arise in miniaturizing the sensors, and various optimizations to provide smaller, lower power, lower cost sensors are discussed. The architecture of the early prototype platform of LaserSPECks (v1.0) and an update (v2.0) is reported in Section 5. A number of novel applications enabled by the sensor platform are discussed in Section 6. Performance evaluation of the LaserSPECks platform in detecting CO_2 is described in Section 7. Finally, we conclude the paper in Section 8.

2. BACKGROUND – OPTICALLY BASED GAS DETECTION

The principle of optical gas detection techniques can be understood via a simple example. The most straightforward method in measuring pollution of an air sample is to expose the sample to a light source and observe the sample with the naked eye; if the sample is not optically clear, it must contain other materials (i.e. smog, fog, smoke, dust) besides pure air. By measuring the exact amount of light absorption associated with each contaminant material, one would gain the ability to distinguish the type and amount of each pollutant. Due to their specific molecular structures, most molecular compounds in the gas phase have spectral absorption *fingerprints* in the infrared (IR) region of light, making them completely distinguishable from each other, effectively guaranteeing the measurement is targeting the correct gas and avoiding interference with other molecules (*specificity*). The basic technique used to perform absorption spectroscopy shines a source of "fingerprint wavelength" light through a sample and detects the percentage of light remaining. This technique is more commonly referred to as *direct absorption spectroscopy*.

The degree to which the compound will absorb a certain wavelength is calculated using Beer-Lambert's law:

$$I(\nu) = I_0 \cdot e^{-\alpha(\nu)L} \quad (1)$$

where I is the intensity of light passing through the absorbing medium, I_0 is the input intensity, L is the optical pathlength through the sample $[cm]$, ν is the radiation frequency in wavenumbers $[cm^{-1}]$, and $\alpha(\nu)$ is the absorption coefficient of specific target species:

$$\alpha(\nu) = C \cdot S \cdot g(\nu - \nu_0) \quad (2)$$

where C is number of molecules of absorbing gas per unit volume $[molecule \cdot cm^{-3}]$, S is the molecular line intensity $[cm^{-1}/(molecule \cdot cm^{-2})]$ and $g(\nu - \nu_0)$ is the normalized lineshape function of molecular absorption $[cm]$, which can be Lorentzian, Gaussian, or Voigt shaped.

Small-sized gas molecular species with only a few atoms (e.g., CO, CO_2, NH_3) have narrowband absorption coefficient $\alpha(\nu)$, requiring the narrow spectral linewidth (single color wavelength) of a *laser* light source to resolve the spectral feature. By centering on these specific frequencies, *laser absorption spectroscopy (LAS)* provides a high sensitivity method of measuring a target gas concentration, while preserving high specificity.

The line intensity S for each spectral line of a target gas varies throughout the electromagnetic spectrum for each molecule, with COTS telecom lasers available in the near-IR region to reach some of these lines. The near-IR wavelength range extends from $\sim$ 1-3 μm, allowing for ppmv-ppbv (part-per-million by volume to part-per-billion, 10^{-6} to 10^{-9}) sensitivity of the gas concentration. In the mid-infrared (MIR) region, strong line intensities (resonance with the fundamental molecular vibrations) are available within the wavelength range from $\sim$3 to 24 μm, allowing for ppbv-pptv (ppb to part-per-trillion, 10^{-9} to 10^{-12}) sensitivity. Standard humidity sensors measure from percentages to per-mil (10^{-2} to 10^{-3}) absolute humidity. Another useful molecule for points-of-reference is carbon monoxide (CO): pure mountain air in an area far from human activities contains $\sim$126 ppbv (1.26×10^{-9}) verified by laser spectroscopy in [17]. Healthy non-smoking humans exhale 1000-3000 ppbv of CO [10] and a lethal dose of CO is 800,000 ppbv for 2 hours.

To increase the optical absorption by the gas (i.e., to increase the signal-to-noise ratio (SNR)), multipass cells (MPC) increase the optical pathlength L by providing 100+ bounces between mirrors for the beam. Usually 100 m of pathlength is effective to quantify ppbv-pptv concentrations in the mid-IR. However, these cells must be manufactured to high tolerance to achieve good performance, may cost \$10k+ USD, and are bulky. Thus far, direct absorption sensors are not currently suited to low-cost miniature sensing.

Another technique (besides direct absorption) that also employs the spectral absorption to measure gas concentrations is photoacoustic spectroscopy (PAS). Sensors based on PAS can withstand much lower tolerance in construction, and can be designed compactly. Unlike direct absorption LAS which relies on measuring relative intensities of light, PAS exploits heating of the sample when the incident radi-

ation is absorbed by the gas. Specifically, modulation of the radiation at audio frequencies produces periodic heating in the gas sample which is detectable by an acoustic transducer (i.e. microphone). The gas chamber is an acoustic resonator that efficiently holds the energy generated by the target gas in the system measured by the quality factor:

$$Q = \frac{f_0}{\Delta f_{\sqrt{2}}} \quad (3)$$

where, for the transfer function of acoustic signal versus frequency, f_0 is the resonant frequency of the resonator, and $\Delta f_{\sqrt{2}}$ is the full-width at $\sqrt{2}$ max points of the resonance. Q is a figure of merit since the signal generation is proportional to Q and typical values for acoustic resonators are $\sim$ 20-200. Higher Q's hold the energy input longer within the system, thus using the excitation energy more efficiently.

3. THEORY OF OPERATION - QUARTZ-ENHANCED PHOTOACOUSTIC SPECTROSCOPY (QEPAS)

Quartz-enhanced photoacoustic spectroscopy (QEPAS) is a variation of PAS that was developed by Kosterev et al. [3] at Rice University in 2002. Instead of storing the energy in a low-Q acoustic chamber and measuring with a microphone, QEPAS uses a high-Q quartz crystal tuning fork (TF) to retain the acoustic energy, while simultaneously acting as the acoustic detector. Typical Q for standard 32,768 Hz tuning forks is about $\sim 10^4$-10^5.

The typical QEPAS implementation involves generating a modulated laser beam which passes between the prongs of the TF. Modulation of the optical frequency is matched to a harmonic of the TF resonant frequency, typically $\frac{f_0}{2}$, where f_0 is the fundamental frequency of the TF of $\sim$32 kHz. The acoustic sound waves generated by periodic heating of the gas sample push the TF prongs apart, generating a current in the piezo-electrically active crystals. In the near-IR, optical fiber coupled telecom components are available to robustly deliver the radiation between the prongs, reducing the effect of mechanical disturbances which cause optical misalignment. An acoustic microresonator consisting of two miniature tubes on opposite sides of the TF in line with the beam may be used to enhance the signal [3].

The TF generates nano-Ampere (nA) level piezo-currents, detectable using a transimpedance amplifier. Lock-in demodulation detects the amplitude of the signal at a reference frequency. Various gases have been measured via QEPAS in previous literature; these results are summarized in Table 1.

The advantages of QEPAS for miniature networked sensors compared to standard LAS and PAS are: (1) miniature sensing element; (2) background free; (3) low cost, (4) noise immune.

QEPAS can use standard mass produced tuning forks which are 4+ orders of magnitude smaller in size than other absorbance detection module (ADM). For example, a 36 m optical path multipass cell from Aerodyne Inc. has dimensions 300×80×100 mm^3, while a standard TF is less than 4×1×3 mm^3.

QEPAS also has marginal background interference and investigations are underway to use QEPAS with broadband absorbers (i.e. explosives, chemical and biological weapons, and chlorofluorocarbons). Lowering the gas pressure improves the sensitivity 2-3×; however, standard pumps are undesirable in long-term field sensors since they are bulky, draw 5-10W+, and have moving parts. Background free measurements for QEPAS sensors allow operation at ambient pressures for pump-free operation, lowering overall system cost, size, and power consumption.

Suitable TFs are readily obtainable and mass produced since they are the timing element for quartz wrist watches and electronic oscillators. At less than $0.30 (USD) each, the quartz TF sensing element has a marginal cost.

Additionally, QEPAS has high noise resistance, suitable for use in high noise and vibration environments (volcanoes, vehicles, and industrial environments). Excitation that does not push the TF prongs apart does not generate a signal, thereby providing noise immunity and high stability. Studies in [6] revealed stability of QEPAS for up to 3 hours of averaging time in a laboratory setting.

3.1 Suitable Lasers

The lasers used in our prototype system are off-the-shelf telecom diode lasers (such as JDS Uniphase CQF93x or NEL-NTT NLK series). However, we emphasize that any compact, tunable light source at the target wavelength which does not need liquid nitrogen cryogenic temperatures or other consumables would be useful. A convenient laser type is the vertical cavity surface emitting laser (VCSEL) which has high efficiency and low cost. Increased node density would make up for the low output optical power. Another suitable type of laser for future implementations will be quantum cascade lasers (QCLs) in the MIR; they will increase output optical power and provide target wavelengths with absorption line-strengths S that are one or more orders of magnitude higher than the NIR telecom region, allowing for improved sensitivities. Once specific application demands increase, QCLs may be mass produced by any company with semiconductor fabrication capability, and directly integrated to our platform.

4. MINIATURIZATION OF QEPAS FOR SENSOR NETWORKS

Although the sensing element is less than 1 cm^3 in volume (Fig. 2), various issues exist preventing a QEPAS-based sensor node from immediate miniaturization to "mote" size and power consumption. The issues are as follows.

1. Integration of laser wavelength control
2. Handling laser power fluctuation
3. Alignment of optical system
4. Handling phase shift from molecular relaxation
5. Handling resonance drifts in the tuning fork
6. Power efficiency and noise

To address these issues, we have developed LaserSPECks v1.0, an early prototype for a WSN gas sensing node architecture that can integrate the necessary circuitry and physical modules for QEPAS. The following is a detailed analysis of the six issues mentioned above.

4.1 Laser Wavelength Control

The laser wavelength must be controlled precisely to match the wavelength of a single spectral line. Typical distributed feedback (DFB) lasers possess a wavelength versus temperature dependence. Outdoor sensors would experience temperature variations which are enough to shift the emission

Molecule (Host)	Frequency, cm^{-1}	Pressure, Torr	NNEA, $cm^{-1}W/Hz^{½}$	Power, mW	NEC (τ=1s), ppmv
H_2O (N_2)**	7306.75	60	1.9×10^{-9}	9.5	9×10^{-2}
HCN (air: 50% RH)*	6539.11	60	$< 4.3\times10^{-9}$	50	1.6×10^{-2}
C_2H_2 (N_2)**	6529.17	75	$\sim 2.5\times10^{-9}$	~ 40	6×10^{-2}
NH_3 (N_2)*	6528.76	60	5.4×10^{-9}	38	0.5
CH_4 (N_2)*	6057.09	700	5.2×10^{-8}	17.6	3.0
CO_2 (exhaled air)	6514.25	90	1.0×10^{-8}	5.2	1×10^{4}
CO_2 (N_2+1.5% H2O) *	4991.26	50	1.4×10^{-8}	4.4	18
CH_2O (N_2:75% RH)*	2804.90	75	9.1×10^{-9}	6.5	0.14
CO (N_2)	2196.66	50	5.3×10^{-7}	13	0.5
CO (propylene)	2196.66	50	7.4×10^{-8}	6.5	0.14
N_2O (air+5%SF_6)	2195.63	50	1.5×10^{-8}	19	7×10^{-3}
C_2HF_5 (Freon 125)***	1208.62	770	2.6×10^{-9}	6.6	3×10^{-3}

Table 1: Previous results for trace gas measurements using QEPAS at Rice University, *=improved microresonator, **=improved microresonator and double optical pass, *=amplitude modulation and metal microresonator, NNEA=normalized noise equivalent absorption coefficient, NEC=noise equivalent concentration, 1 sec., Measurement of CO_2 in exhaled air with NIR wavelengths was described in [24].**

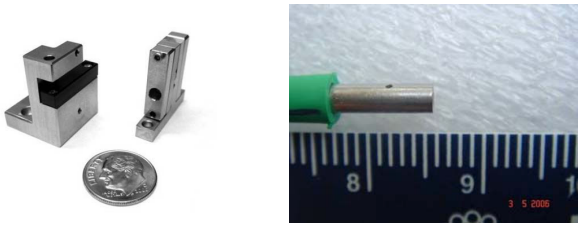

(a) (b)

Figure 2: (a) Alignment tool, US Dime, Absorbance Detection Module (ADM); (b) A miniature fiber collimating lens.

wavelength away from the gas absorption line. The electrical bias current through the laser produces Joule heating (current through a resistive element) which also heats the laser, further complicating wavelength control. Typically, a proportional-integral-derivative (PID) controller provides the temperature control loop, while another feedback loop controls the current to stabilize the optical wavelength. Telecom lasers commonly integrate a Peltier thermo-electric cooler (TEC) into the laser packaging, but control electronics require printed circuit board (PCB) area. Additionally, the TEC requires a heatsink to pump heat away from the laser substrate, and a reference cell (also COTS in the telecom industry) filled with a reference concentration of the target gas provides a wavelength target, further occupying PCB area. Using the main microcontroller to perform PID compensation calculations saves space which might have been used for analog compensation, and using large copper pours on multiple PCB layers lowers required heat sink area due to a larger thermal mass. Temperature control is required in many other types of sensors; therefore, advanced WSN platforms should accommodate with suitable interfaces and appropriate physical space.

4.2 Laser Power Fluctuations

The PAS signal is proportional to the optical power. Although photodiodes are usually integrated into telecom lasers to measure output power, normalization (via division) is an expensive operation in the fixed point hardware typically used in WSNs. By using a look-up table (LUT) and a hardware multiplier to do inverted multiplication (instead of direct division), the system performs normalization faster to allow for higher bandwidth noise reduction. More space for memory and a processor that has a hardware multiplier results in a large PCB footprint and a higher cost.

4.3 Alignment of Optical System

The gap of a typical tuning fork is 0.3 mm wide. Thus, optical alignment equipment requires a large volume to handle micrometer translation and rotation stages. To avoid this issue, a permanent alignment system is required. In Fig. 2a, the alignment tool sets the TF to a known position, to be inserted into the ADM, and placed on a mount with an aligned collimating lens (Fig. 2b).

4.4 Phase Shift from Molecular Relaxation

Lock-in amplifier (LIA) detection detects the PAS signal. This method extracts the signal using phase sensitive detection at a specific frequency based on a reference local oscillator. LIA techniques are homodyne detectors, down-converting the target frequency content to DC. Molecular vibrational-translational (VT) relaxation effects [5] [28] in QEPAS cause the signal to phase shift in the presence of relaxer molecules (H_2O is a strong relaxer). Since the signal can shift to a continuous number of angles, the system must either sample at a high analog-to-digital converter (ADC) sampling rate to assure efficient detection, or use an analog LIA scheme. Although currently available ADCs are fast and low power, processing the stream of information is not straightforward with low-power processors. In our prototype, we use analog quadrature detection (90° phase shifted references) to relax requirements on signal processing.

4.5 Resonance Drifts in the Tuning Fork

The resonance frequency and Q factor of the TF is dependent on pressure. The modulation frequency and LIA reference frequencies need to be varied over a 0.1 Hz range

if ambient pressure changes 10 Torr, and the frequencies need to be tuned within 0.01 Hz due to the high Q. To address this issue, we develop a method to generate 5 ultrasonic synchronized waveforms ($\frac{f_0}{2}$, f_0, $f_0+\frac{\pi}{2}$, $\frac{3f_0}{2}$, $\frac{3f_0}{2}+\frac{\pi}{2}$) to perform $2f$ quadrature detection and $3f$ quadrature line-locking with low overhead; the method is as follows.

1. Generate a single sinusoidal waveform using direct digital synthesis (DDS) at a multiple of all of the waveform frequencies ($12f_0$);
2. Remove output DAC sampling rate by low pass filtering;
3. Use a comparator to convert the signal to a square waveform;
4. Use digital counters to divide the signals into their respective frequencies;
5. Further changes in frequency can be controlled simultaneously using the single phase accumulator;

The MSP430F1611 implemented in our platform has an integrated DAC, comparator, and asynchronous digital counters; thus, the only missing component is a low pass filter. Voltage controlled oscillators (VCOs) such as the Linear Technologies LTC1799 could be used to produce the $12f_0$ signal in a smaller package; however, providing a circuit to set the frequency at ppm accuracy to account for the high Q of the TF (less than $1Hz/196608Hz$) would be comparable in cost, size, and power consumption to a second MSP430 performing DDS.

The same divided signal method can provide better results in a digitally implemented LIA (for a high speed DSP) via the same DDS $12f_0$ generation using a single phase accumulator, and using parallel LUTs for each synchronized frequency reference to reduce overhead.

4.6 Power Efficiency and Noise

The sensor consumes up to 800mA for a high power telecom laser diode. In our first prototype version (LaserSPECks v1.0), bias current was provided by class A amplifiers, with typical efficiencies of <50%. The high currents (due to the inefficiency) must be placed physically away from the sensitive analog electronics since they are modulated at a harmonic of the target frequency for the LIAs. A linear output amplifier (class A, B, or AB) provides low noise for large bandwidths, but low efficiency. Increasing efficiencies via switching supplies and "class D" amplifiers in the next version of the boards (v2.0) will lower the amount of current in the current loops, minimizing unnecessary antenna power. The electromagnetic interference (EMI) generated due to the class D switching of the system is not efficiently detected by the LIAs, since they are not a harmonic of the resonant frequency and are two orders of magnitude higher in frequency. Switching power supplies generate ripple current on the output, which is generally filtered by an LC filter. Class D amplifiers for laser bias are not generally considered for non-pump laser-based systems since telecom lasers operate at high data rates (50Mbps-10Gbps) where ripple in voltage or current would cause errors.

Assuming a f_o output frequency modulation with a suitable LC filter at 16kHz and a switching frequency f_s of 3MHz, the attenuation according to [20] is:

$$|H_{LP}|_{dB} = -40log(\frac{f_s}{f_o}) \quad (4)$$

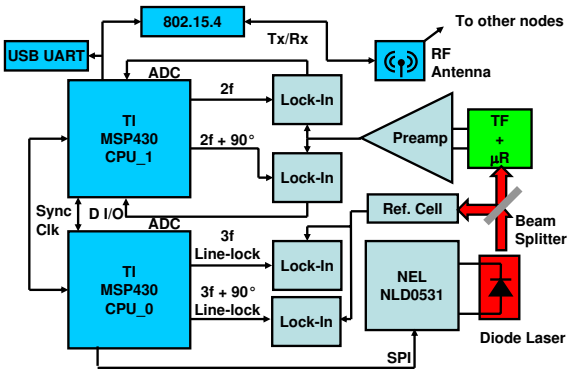

Figure 3: Block diagram of LaserSPECks v1.0 for QEPAS. TF = Tuning fork, μR = Microresonator

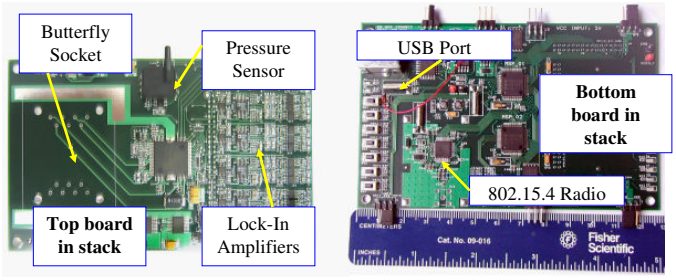

Figure 4: LaserSPECks v1.0 based on GNOMES 3.0. The sensor integrates 2 MSP430 processors and a CC2420 ZigBee radio.

which is ~ -90 dB attenuation for the parameters above, enough to prevent spectral linewidth broadening due to current ripple in the laser. Converting a switching voltage regulator to a switching current source has been described in [19].

5. LASERSPECKS SENSOR PLATFORM ARCHITECTURE

The LaserSPECks platform implements a dual MSP430-F1611 platform plus Chipcon CC2420 based on the GNOMES (Generalized Network of Miniature Environmental Sensors) 3.0 platform [25]. The GNOMES platform was first developed in 2002 using a MSP430F149 and a Bluetooth radio. The first generation of QEPAS controller using GNOMES 3.0 was designed to handle 5 synchronized independently phase tunable DDS sine wave outputs, using 4 digital to analog converters (DACs) (from the 2 MSP430s) and 1 serial peripheral interface (SPI) DAC integrated into a laser control module NEL NLD0531 (Fig. 3). While not measuring, one MSP430 performed the communications functions, while the other performed calculations on the sampled data. A photograph of the current LaserSPECks v1.0 design (described above) is illustrated in Fig. 4.

LaserSPECks v2.0 will be the second generation, which integrates the two boards into one board, will use custom class D laser and TEC drivers, and will use all of the improvements to efficiency listed in this work. The system provides more efficient generation of LIA and laser current modulation reference waveforms. The LIA and laser control subsystems will draw about 70 mA (without the laser

or TEC) in measurement mode for the simulated system in Table 2.

Specialized microcontroller features used in the v1.0 LaserSPECks are: a hardware multiplier to generate arbitrary amplitude sine waves, flash memory to hold a sinusoidal LUT and a normalization LUT, a DAC to perform high bandwidth line-locking current corrections, SPI bus to provide commands to a NEL NLD0531 TEC+laser PID controller, and DACs to generate 5 independent DDS sine waves.

The Berkeley/Moteiv Telos mote [13] and the GNOMES platform share similar MSP430 + CC2420 architectures. The system could either add another MSP via daughtercard connected on a bus, or replace the functionality with stand alone DDS ICs or clock generators and use the Telos as the main processor to achieve the same performance.

The sensor architecture is abstracted to work with both LAS and PAS in continuous wave (CW) $2f$ modulation detection, so various types of networked trace-gas monitoring can be implemented. Perimeter monitoring is one such networked/sensing architecture, where the lasers are sent between nodes to find the integrated absorption along the path the beam takes. However, any large debris or temporary blockage of the beam results in measurement errors, and node failure causes a greater loss of data (loss of entire area between 2 points as opposed to an area covering one point. Note, the majority of networked sensing applications of LaserSPECks do not need direct laser contact between the nodes such as the ones used in perimeter monitoring. This is so, because the nodes can use the wireless network to exchange local point sensor data without the need for direct beam forming of the data, while distributed signal processing techniques can be exploited to draw conclusions about the spatio-temporal properties of the gas dynamics.

Multipass cells (MPCs) also work with the sensor architecture, and in fact would draw much less power. MPC-LAS is ideally independent of optical power, since its measurements are based on the ratio of intensities. There is no resonant frequency in direct absorption, so DDS is unnecessary, allowing much lower system clock rates (power dissipation in CMOS scales with clock rate). The system can measure with much less power, although there is an overhead in cost, as the MPC unit is currently expensive to manufacture (large optical surfaces).

A novel, useful sensing mode could operate the sensor in a low power mode via short path LAS or perimeter monitoring and then switch to QEPAS for high resolution, or implement a combination of both with the proper network control and data mining techniques.

Integrated Circuit	qty	Current [A]
MSP430F1611	2	0.0133
AD8615	3	0.0051
ADG619	2	0.0000
AD623	3	0.0000
AD8618	3	0.0204
ADG734	1	0.0000
DRV592	2	0.0140
INA330	1	0.0026
MAX5401	1	0.0000
DAC8831	2	0.0000
LT1563-2	1	0.0080
	Total:	0.0635

Table 2: Integrated circuits involved in measurement mode, rounded to 10^{-4} A.

6. APPLICATIONS OF NETWORKED GAS SENSING

Until recently, as mentioned above, trace-gas sensing has been limited to single point measurements due to the size and costs of sensors capable of accurately detecting a target gas species. Generally, the goal of networking gas sensors is to provide source and sink localization, flux measurements, and forecast predictions of gas concentrations over a wide area. A selection of the many possible applications are:

1. Industrial monitoring in semiconductor, petroleum, and pharmaceutical applications
2. Agricultural monitoring and livestock health
3. Environmental monitoring for carbon sources and sinks, volcanic emissions monitoring
4. Health and safety monitoring to detect nearby hazard areas or determine quarantine targets, personal area networks, and breath analysis
5. Security applications such as explosives sniffing, or biowarfare agent mapping

A brief exploration of each group of applications and some examples follow:

One example of a novel use for trace-gas sensors within WSNs is monitoring of ammonia in semiconductor foundries. Based on our ongoing discussions with Texas Instruments and Motorola, ammonia [NH_3] is one contaminant gas which must be monitored closely to avoid multi-million dollar yield failure. The measurement is currently performed by a large $40k ion-mobility spectrometer (non-optical) measuring ppbv levels and checked hourly. A multipoint system was described in [8] and reported a resolution of 143 pptv (0.1 $\mu g/m^3$) and recommended taking data in 160 minute intervals using ion-chromatography. QEPAS has shown a detection limit of 650 ppbv in 1 second using a telecom laser [6]; at 160 minute intervals this provides 6 ppbv resolution which is only an order of magnitude away from the required detection sensitivity, achievable with a fiber amplifier [22] to increase power, or a QC laser [4] to reach stronger line intensities. The petroleum and pharmaceutical industries also have need for multipoint contamination monitoring. With large volumes to monitor, mapping precisely to search for sources of the target contaminant can provide invaluable information to plant facilities managers. Taking advantage of their low power consumption and miniature size, these sensors can be deployed without major renovations of infrastructure.

The LaserSPECks platform may also improve agriculture and food production. Improving monitoring in areas which cannot afford to lose crops would greatly help in improving yield while lowering environmental impact. Rice is the staple food source of many countries, and monitoring methane (CH_4) may indicate a lack of flooding and impending crop failure. Previously, a method using satellite radar imagery was used to monitor rice growth over a large area in [21] to monitor methane production. Monitoring sections of land in a network can allow farmers to pinpoint problems before losses occur.

Environmental monitoring to measure carbon sources and sinks will gauge the impact of greenhouse gases such as CO_2 and methane on climate. Research has been ongoing in underground carbon sequesterization and leaks of these greenhouse gases can be monitored continuously. High precision measurements of atmospheric flux by airplanes flying cross patterns with onboard instrumentation, can be replaced with stationary networked sensors to provide continuous real-time information. Additionally, adoption of the Kyoto Protocol and future environmental treaties will require detection of unauthorized random emission of greenhouse gases, difficult to detect with single point measurements. Volcanoes are also of interest [12, 26] to link various emissions to activity and emissions to the atmosphere. Currently, volcanic emissions researchers put on fire suits to take samples on location. The ability to deploy multiple environmentally hardened sensors which operate without human intervention will greatly improve data gathering.

These sensors can also perform breath analysis to diagnose and monitor diseases, providing powerful new personal area network (PAN) applications. Recently, nitric oxide (NO) breath analysis has been FDA (US Food and Drug Administration) approved to diagnose asthma. Nitric oxide is a biomarker molecule for inflammation, and becomes elevated for asthma, chronic obsructive pulmonary disease, and influenza. Research has shown links in acetaldehyde [C_2H_4O] [16] and formaldehyde [HCHO] to cancer. Various other biomarkers and their associated diseases are listed in Table 3. One feasible application is for diabetes breath monitoring. Instead of blood tests, or implanted testers, periodic breath tests into a handheld device would provide adequate information for an automated insulin delivery system on the personal area network to activate. Furthermore, data targeting environmental factors can be uploaded to medical researchers in order to determine causes for various conditions, such as autism, asthma, and cancer. Ongoing collaborations within the MIRTHE ERC with the Johns Hopkins Bloomberg School of Public Health have focused on improving exhaled breath analysis, and also for developing instrumentation based on optical techniques. We have previously explored breath analysis in [9] for nitric oxide [NO] relationships to chronic obstructive pulmonary disease (COPD) and in [29] for carbonyl sulfide [COS] relationships to lung transplant rejection (both in collaboration with the Texas Medical Center). We stress that these applications are only enabled through high specificity, high resolution, miniature sensors - the objective of this work.

Security applications enabled by the LaserSPECks platform include providing drug and bomb sniffing capabilities, detection of biological warfare agents, and search and rescue operations. Acetone [CH_3COCH_3] mixed with hydrogen peroxide [H_2O_2] creates triacetone triperoxide [TATP], used in the London subway bombings and during the 2006 transatlantic aircraft plot on a flight from London to the United States. Monitoring all of the constituents and end products in a network will provide more powerful screening than single point sensing at a security entrance. Freon-125 [C_2HF_5] detection, has provided proof-of-concept QEPAS measurements of larger molecules possessing broadband absorption spectra (which mimic explosives and biological agents) [27]. Freon-125 is used as a simulant of DIMP [diisopropyl methylphosphonate], a byproduct of sarin nerve gas production. Biological warfare agent mapping may also provide assistance during gas attacks like the Tokyo subway sarin gas attack to direct those in the vicinity to the correct exits. In search and rescue operations, people trapped under debris can be detected by localization of waste ammonia which is generated by the victims using a sensor network. Such sensing will greatly speed location of the victims compared to using dogs walking over unstable debris.

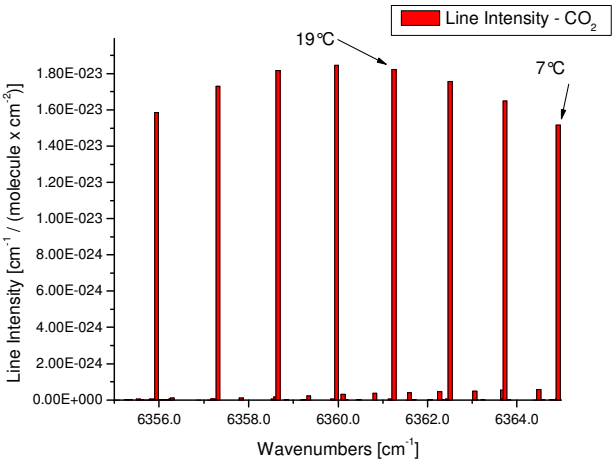

Figure 5: Line intensity for the spectral region around 6361.0 cm^{-1}. The line 19°C was used for experimental measurements.

Low power, ultra compact, high specificity trace-gas sensing has been explored previously. Mulligan et al. at Purdue University has developed a shoe box sized mass spectrometer which weighs 10 kg [11]. In 2004 Webster et al. at NASA Jet Propulsion Laboratory (JPL) [23] described a laser based absorption implementation for a Mars rover which weighed 230g, and drew 0.96A scaled to 3V and had a detection limit of 1 ppm for water vapor. Southwest Sciences recently developed a system for CO_2 to fly on atmospheric weather balloons, which drew 1.3A scaled to 3V using a 2μm VCSEL in direct absorption, and weighed 1 kg [15]. Note that LaserSPECks has the potential for lower cost and smaller footprint than other trace-gas sensing methodologies for similar sensitivity; LaserSPECks is also the first reported integration of trace-gas sensors within a wireless computing node suitable for WSNs applications.

7. EXPERIMENTAL RESULTS

This work has resulted in a working prototype for CO_2 sensing which is based on QEPAS and LaserSPECks v1.0. The system was applied to measure CO_2 at 1.5 μm optical wavelength using a standard distributed feedback (DFB) telecom diode laser (CQF935/908, JDS Uniphase). Setting the laser bias to 150 mA, the voltage across the laser requires 1.25 V, and provides 26 mW of optical power. The TEC required 80 mW to take the laser substrate from room temperature to 19 °C. These settings caused the laser to emit radiation at 6361.2509 cm^{-1} wavenumbers (1.572 μm) as demonstrated in Fig. 5.

A beam splitter coupled to a reference cell allowed for line locking and power normalization. An acoustic microresonator was also installed with the tuning fork. The embedded MSP430 12-bit ADCs were used to sample the signal.

Molecule	Formula	Biological/Pathology Indication
Pentane	$CH_3(CH_2)_3CH_3$	Lipid peroxidation, oxidative stress associated with inflammatory diseases, immune response, transplant rejection, breast and lung cancer
Ethane	C_2H_6	Lipid peroxidation and oxidative stress
Carbon Dioxide isotope ratio	$^{13}CO_2$ / $^{12}CO_2$	Marker for Heliobacter pylori infection, GI and hepatic function
Carbonyl Sulfide	COS	Liver disease & acute rejection in lung transplant recipients
Ammonia	NH_3	Hepatic encephalopathy, liver cirrhosis, fasting response
Formaldehyde	HCHO	Cancerous tumors, breast cancer
Nitric Oxide	NO	Inflammatory and immune responses (e.g., asthma) and vascular smooth muscle response
Hydrogen Peroxide	H_2O_2	Airway Inflammation, Oxidative stress
Carbon Monoxide	CO	Smoking response, CO poisoning, vascular smooth muscle response, platelet aggregation
Ethylene	$H_2C{=}CH_2$	Oxidative stress, cancer
Acetone	CH_3COCH_3	Fasting response, diabetes mellitus response, ketosis

Table 3: A number of biomarkers for various human diseases and health states.

A DDS system was developed to generate waveforms for the laser modulation, and $2f$ and $3f$ quadrature LIA local oscillators, to match the resonant frequency of the TF. Two 16-bit registers were used as a 32-bit phase accumulator for each frequency and phase. Each cycle through the software's measurement loop added a phase increment to the phase accumulator, and then compared the angle to a LUT for the correct DAC output value. Using the MSP430 built-in digitally controlled oscillator (DCO) or using any other resistive-capacitive (RC) tunable clock source to match to the TF would degrade the bandwidth of the temperature and current control loops if linked to the system clock. Using the DDS method, a TF resonance scan (laser off, frequency of lock-in swept) was used to measure the resonance frequency f_0 and bandwidth $\Delta f_{\sqrt{2}}$ to determine Q of a TF open to ambient air. The resistance of air causes the Q factor to fall, and causes the bandwidth to widen to ~ 4 Hz. Q will fluctuate in field experiments, and the system must quickly tune to the correct frequency, to account for the varying Q. Quick tuning is possible in a clock cycle by changing synchronized DDS phase accumulators.

The measure of the minimum absorption coefficient $\alpha(\nu)$ that is measurable before the signal-to-noise ratio (SNR) of the measurement reaches 1 is the normalized noise equivalent absorption coefficient (NNEA). With more power and longer averaging times, the minimum $\alpha(\nu)$ detectable improves – directly with power, and with a $\sqrt{\tau}$ dependence for averaging time. The HITRAN (HIgh-resolution TRANsmission molecular absorption database) [14] is a spectral databases which contains information on absorption coefficients for various compounds (Fig. 6).

The spectrum in Fig. 7 shows the system measuring a sample of 100% CO_2 at pressure of 90 Torr with a $9.75{\times}10^{-4}$ s lock-in time constant. The SNR was 72.4 for 1σ (standard deviation) noise, resulting in a 1.38% detection sensitivity. This provides an minimum $\alpha(\nu)$ detectable for 1.38% CO_2 of $1.19{\times}10^{-5}$ cm^{-1} according to HITRAN. Narrowing the detection bandwidth to 1 Hz provides noise reduction to reach minimum $\alpha(\nu)$ of $6{\times}10^{-7}$ cm^{-1} , allowing the sensor to achieve a NNEA of $1.59{\times}10^{-8}$ cm$^{-1}\cdot$ W/ $\sqrt{Hz}$, or 410 ppb in 1 second, which is comparable to the previous literature in Table 1. Ambient concentration of CO_2 is currently 300 ppm, achievable in 4 seconds through by means of averaging.

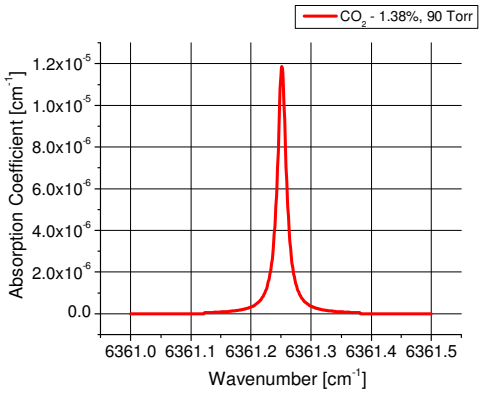

Figure 6: Absorption coefficient for 1.38% CO_2 from HITRAN database.

Integrated multi-frequency lock-in detection using a DSP processor has been described by Sonnaillon et al. in [18]. Their system used a 40MHz pipelined DSP and could measure 3 independent channels with frequencies up to 20 kHz. Assuming the use of the Analog Devices ADSP-21061L, the best low power case at 3.3V at 40 MHz draws 225 mA. $2f$ modulation spectroscopy with line locking for QEPAS requires 4 channels - 2×32 kHz and 2×49 kHz - plus generation of a 16 kHz laser control voltage. The signal generation was provided by two 8 MHz MSP430s with analog mixers for demodulation. The LaserSPECks v1.0 sensor draws 500 mA at 3.3V for the multi-frequency 4 independent channel lock-in with frequencies up to 49 kHz, using 4 × Analog Devices AD8343 2.5 GHz mixer with a single ended clock, with 8 × AD8203 amplifiers, and 8 × MAX742x active filters. This configuration assures minimal bandwidth restrictions, but draws a great deal of supply current. Digital sampling bandwidth necessary would be approximately the maximum $3f$ 49152 Hz × 2 for the Nyquist criterion × 2 quadrature phases × 10 for minimal aliasing = 1.97 MHz (too fast to acquire data from an I^2C or SPI bus and processing stream data digitally with the MSP430).

Fig. 8 shows the difference between an analog and digital LIA phase sensitive detection implementation. Analog LIAs use switching to rectify the signal using analog cir-

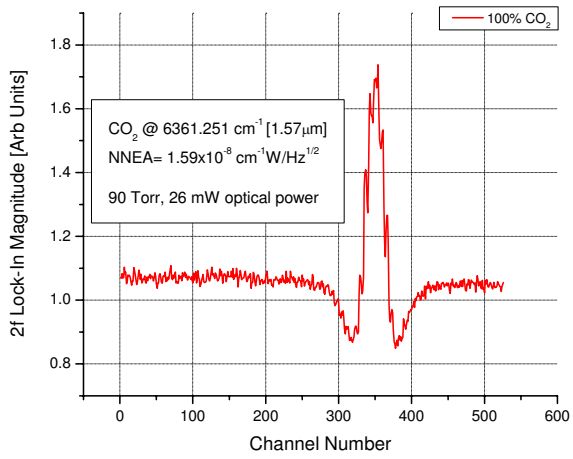

Figure 7: Spectral $2f$ measurement for CO_2. LaserSPECks v1.0 reached 1.19x10^{-5} cm^{-1} absorption coefficient for 9.75x10^{-4} s LIA time constant and 26 mW of optical power in a handheld package.

cuitry. Digital LIAs multiply the sampled waveform by the reference waveform digitally. Thus, digital LIAs are usually higher performance due to the lack of odd-order harmonics from analog square wave multiplication. The differences between analog and digital LIA performance are explored in detail in [7]. Analog multipliers which can directly multiply two analog signals without switching are not commonly used in consumer electronics, and currently do not have small IC package footprints, although low power analog multipliers have been explored in [1] for large-scale integration. Lock-in detection is useful in many other scientific measurement applications; thus, the miniature low-power, multi-frequency lock-in detection described here will be of use to many sensor types other than gas sensors.

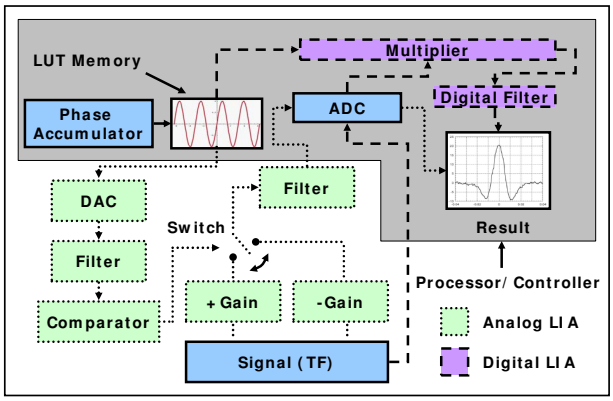

Figure 8: Examples of single channel lock-in detection using DDS in an analog (switching between +G, -G at target frequency) and digital method (digitally multiplies by target frequency).

Although the v1.0 sensor performed to expectations, an upgrade to the system in progress will improve sensor performance further. Version v2.0 of LaserSPECks provides improvements to noise and efficiency. This update will measure improvements from fully synchronized reference waveforms, a balanced demodulator (instead of AD8343 in single ended clock mode), higher resolution to the laser current modulation and offset (instead of a 12 bit DAC), and minimizing high power current loops. These improvements will result in lowering the total analog LIA power usage to 70 mA. Version 2.0 will also further explore sensor miniaturization and preliminary tests reveal a weight of <100 g with a 1.3 mAh Li-Ion battery. Costs will be $2k per node for lasers capable of 40mW in the NIR. These sensors may eventually cost <$100 per node with suitable advances in laser manufacturing and increases in application demand.

8. CONCLUSIONS

We have developed miniaturized, low-power QEPAS, the first high-resolution high-specificity trace-gas sensing technology that is practical for real-world integration into nodes in WSNs. Such sensor nodes will allow for numerous, novel applications of gas sensing in a wide variety of research and industrial fields. The same device can be adapted to detect and quantify numerous gas species at ppmv-ppbv concentrations simply by changing the wavelength of the laser. No human interaction is required, since these sensors are maintenance free, robust, and false-positive resistant, desirable in multi-node networks. These sensors also have high sensitivity and specificity; they quantify gases with high precision and reliability, with orders of magnitude reduction in size, cost, and power consumption compared to the presently available technology for high-performance trace-gas sensing.

LaserSPECks v1.0, an early prototype of the sensors integrated within a wireless platform was built from COTS components. We described the utility of optically based gas sensing techniques, issues that arise in designing and realizing the sensors, as well as our efforts to address the engineering issues to adapt them to WSNs. Experimental evaluations with carbon dioxide, an important greenhouse gas, serves as a proof-of-concept for the successful design and integration of a miniature trace-gas sensor with the capability of sensing 410 ppb for CO_2 in 1 second in the NIR. A newer version of the platform, LaserSPECks v2.0, is under way; the goals of v2.0 are to exceed version v1.0 in terms of miniaturization, power consumption, and cost.

9. ACKNOWLEDGEMENTS

The authors gratefully acknowledge financial support from the National Aeronautics and Space Administration and the National Science Foundation. The authors acknowledge Sriram Narayanan for testing the ZigBee radio and discussions on sensor network applications, Erik Welsh for developing the GNOMES hardware, Adrian Valenzuela for MSP430 support, Ashutosh Sabharwal and Gerard Wysocki for insightful feedback and comments.

10. REFERENCES

[1] C. Chen and Z. Li. A Low-Power CMOS Analog Multiplier. *IEEE Trans. Circ. Sys. II*, 53(2):100–104, 2006.

[2] R. Curl and F. Tittel. Tunable infrared laser spectroscopy. *Annu. Rep. Prog. Chem. C*, (98):217–270, 2002.

[3] A. Kosterev, Y. Bakhirkin, R. Curl, and F. Tittel. Quartz-enhanced photoacoustic spectroscopy. *Opt. Lett.*, 27:1902–1904, 2002.

[4] A. Kosterev, Y. Bakhirkin, and F. Tittel. Ultrasensitive gas detection by quartz-enhanced photoacoustic spectroscopy in the fundamental molecular absorption bands region. *Appl. Phys. B*, (80):133–138, 2005.

[5] A. Kosterev, T. Moseley, and F. Tittel. Impact of humidity on quartz-enhanced photoacoustic spectroscopy based detection of HCN. *Appl. Phys. B*, (85):295–300, 2006.

[6] A. Kosterev, F. Tittel, D. Serebryakov, A. Malinovsky, and I. Morozov. Applications of quartz tuning forks in spectroscopic gas sensing. *Rev. of Sci. Instr.*, 76(043105), 2005.

[7] A. Mandelis. Signal-to-noise ratio in lock-in amplifier synchronous detection: A generalized communications systems approach with applications to frequency, time, and hybrid (rate window) photothermal measurements. *Rev. of Sci. Instr.*, (65):3309, 1994.

[8] Y. Matsuyoshi, Y. Satoh, T. Shinozaki, E. Suzuki, and N. Nagata. High-speed and sensitive multiple-point ammonia gas monitor system. In *Semiconductor Manufacturing Conference Proceedings, 1999 IEEE International Symposium on*, pages 409–412, 1999.

[9] M. R. McCurdy, Y. A. Bakhirkin, and F. Tittel. Quantum cascade laser-based integrated cavity output spectroscopy of exhaled nitric oxide. *Appl. Phys. B*, (85):445–452, 2006.

[10] B. Moeskops, H. Naus, S. Cristescu, and F. Harren. Quantum cascade laser-based carbon monoxide detection on a second time scale from human breath. *Appl. Phys. B*, (82):649–654, 2006.

[11] C. C. Mulligan, D. R. Justes, R. J. Noll, N. L. Sanders, B. C. Laughlin, and R. G. Cooks. Direct monitoring of toxic compounds in air using a portable mass spectrometer. *Analyst*, (131):556–567, 2006.

[12] C. Panichi and G. L. Ruffa. Stable isotope geochemistry of fumaroles: an insight into volcanic surveillance. *J. of Geodynamics*, 32(4–5):519–542, 2001.

[13] J. Polastre, R. Szewczyk, and D. Culler. Telos: enabling ultra-low power wireless research. In *International symposium on Information processing in sensor networks (IPSN), SPOTS track*, page 48, 2005.

[14] L. S. Rothman, A. Barbe, D. C. Benner, L. R. Brown, C. Camy-Peyret, M. R. Carleer, K. Chance, C. Clerbaux, V. Dana, V. M. Devi, A. Fayt, J.-M. Flaud, R. R. Gamache, A. Goldman, D. Jacquemart, K. W. Jucks, W. J. Lafferty, J.-Y. Mandin, S. T. Massie, V. Nemtchinov, D. A. Newnham, A. Perrin, C. P. Rinsland, J. Schroeder, K. M. Smith, M. A. H. Smith, K. Tang, R. A. Toth, J. V. Auwera, P. Varanasi, and K. Yoshino. The HITRAN molecular spectroscopic database: edition of 2000 including updates through 2001. *J. Quant. Spectrosc. Radiat. Transfer*, (82):5–44, 2003.

[15] J. Silver and M. Zondlo. High-precision CO_2 sensor for meteorological balloons. In S. Christesen, A. S. III, J. Gillespie, and K. Ewing, editors, *Optics East*, volume 6378-15, page 63780J. SPIE, 2006.

[16] D. Smith, T. Wang, J. Sule-Suso, P. Spanel, and A. El Haj. Quantification of acetaldehyde released by lung cancer cells in vitro using selected ion flow tube mass spectrometry. *Rapid Comm. in Mass Spectr.*, 77(8):845 – 850, 2003.

[17] S. So, G. Wysocki, J. Frantz, and F. Tittel. Development of DSP controlled quantum cascade laser-based trace gas sensor technology. *IEEE Sensors J.*, 6(5):1057–1067, 2006.

[18] M. O. Sonnaillon and F. J. Bonetto. A low-cost, high-performance, digital signal processor-based lock-in amplifier capable of measuring multiple frequency sweeps simultaneously. *Rev. of Sci. Instr.*, 76(024703), 2005.

[19] S. Strozecki. Switching regulator forms constant-current source. *EDN magazine*, page 92, May 2002.

[20] Texas Instruments. *SLOS390A, DRV592 Datasheet*, 2002.

[21] T. L. Toan, F. Ribbes, L.-F. Wang, N. Floury, K.-H. Ding, J. A. Kong, M. Fujita, and T. Kurosu. Rice crop mapping and monitoring using ERS-1 data based on experiment and modeling results. *IEEE Trans. on Geoscience and Remote Sensing*, 35(1):41–56, 1997.

[22] M. Webber, T. MacDonald, M. B. Pushkarsky, C. K. N. Patel, Y. Zhao, N. Marcillac, and F. M. Mitloehner. Agricultural ammonia sensor using diode lasers and photoacoustic spectroscopy. *Meas. Sci. and Tech.*, 16:1547–1553, 2005.

[23] C. Webster, G. Flesch, K. Mansour, R. Haberle, and J. Bauman. Mars laser hygrometer. *Appl. Opt.*, (27):4436–4445, 2004.

[24] D. Weidmann, A. A. Kosterev, F. K. Tittel, N. Ryan, and D. McDonald. Application of a widely electrically tunable diode laser to chemical gas sensing with quartz-enhanced photoacoustic spectroscopy. *Opt. Lett.*, 29(16):1837–1839, 2004.

[25] E. Welsh, W. Fish, and J. Frantz. GNOMES: A testbed for low-power heterogeneous wireless sensor networks. In *IEEE International Symposium on Circuits and Systems (ISCAS)*, volume 4, pages 836–839, 2003.

[26] G. Werner-Allen, K. Lorincz, M. Welsh, O. Marcillo, J. Johnson, M. Ruiz, and J. Lees. Deploying a wireless sensor network on an active volcano. *IEEE Internet Computing*, 10(2):18–25, 2006.

[27] M. Wojcik, M. Phillips, B. Cannon, and M. Taubman. Gas-phase photoacoustic sensor at 8.41μm using quartz tuning forks and amplitude-modulated quantum cascade lasers. *Appl. Phys. B*, 85:307–313, 2006.

[28] G. Wysocki, A. Kosterev, and F. Tittel. Influence of molecular relaxation dynamics on quartz-enhanced photoacoustic detection of CO_2 at $\lambda = 2\ \mu m$. *Appl. Phys. B*, (85):301–306, 2006.

[29] G. Wysocki, M. McCurdy, S. So, D. Weidmann, C. Roller, R. F. Curl, and F. K. Tittel. Pulsed quantum-cascade laser-based sensor for trace-gas detection of carbonyl sulfide. *Appl. Opt.*, 43(32):6040–6046, 2004.